AFRL-RY-WP-TP-2008-1159

WIGNER-HOUGH/RADON TRANSFORM FOR GPS POST-CORRELATION INTEGRATION (PREPRINT)

Dr. Chun Yang, Dr. Mikel Miller, Dr. Thao Nguyen, and Dr. Erik Blasch

Sigtem Technology, Inc.

SEPTEMBER 2007

AIR FORCE RESEARCH LABORATORY
SENSORS DIRECTORATE
WRIGHT-PATTERSON AIR FORCE BASE, OH 45433-7320
AIR FORCE MATERIEL COMMAND
UNITED STATES AIR FORCE

REPORT DOCUMENTATION PAGE

Form Approved
OMB No. 0704-0188

1. REPORT DATE *(DD-MM-YY)*	2. REPORT TYPE	3. DATES COVERED *(From - To)*
September 2007	Conference Paper Preprint	08 April 2005 – 08 September 2007

4. TITLE AND SUBTITLE
WIGNER-HOUGH/RADON TRANSFORM FOR GPS POST-CORRELATION INTEGRATION (PREPRINT)

5a. CONTRACT NUMBER
FA8650-05-C-1828

5b. GRANT NUMBER

5c. PROGRAM ELEMENT NUMBER
65502F

6. AUTHOR(S)
Dr. Chun Yang (Sigtem Technology, Inc.)
Dr. Mikel Miller (AFRL/MNG)
Dr. Thao Nguyen (AFRL/RYRN)
Dr. Erik Blasch (AFRL/RYAA)

5d. PROJECT NUMBER
3005

5e. TASK NUMBER
13

5f. WORK UNIT NUMBER
300513CY

7. PERFORMING ORGANIZATION NAME(S) AND ADDRESS(ES)
Sigtem Technology, Inc.
1343 Parrott Drive
San Mateo, CA 94402-3630

Advanced Guidance Division (AFRL/MNG)
Air Force Research Laboratory
Munitions Directorate
Eglin AFB, FL 32542

Reference Systems Branch (AFRL/RYRN)
RF Sensor Technology Division
Assessment and Integration Branch (AFRL/RYAA)
Sensor ATR Technology Division
Air Force Research Laboratory, Sensors Directorate
Wright-Patterson Air Force Base, OH 45433-7320
Air Force Materiel Command, United States Air Force

8. PERFORMING ORGANIZATION REPORT NUMBER

9. SPONSORING/MONITORING AGENCY NAME(S) AND ADDRESS(ES)
Air Force Research Laboratory
Sensors Directorate
Wright-Patterson Air Force Base, OH 45433-7320
Air Force Materiel Command
United States Air Force

10. SPONSORING/MONITORING AGENCY ACRONYM(S)
AFRL/RYRN

11. SPONSORING/MONITORING AGENCY REPORT NUMBER(S)
AFRL-RY-WP-TP-2008-1159

12. DISTRIBUTION/AVAILABILITY STATEMENT
Approved for public release; distribution unlimited.

13. SUPPLEMENTARY NOTES
Paper produced under contract FA8650-05-C-1828 for technical report AFRL-RY-WP-TR-2008-1137, SOFTWARE TOOLKIT FOR NONLINEAR FILTERS FOR GLOBAL POSITIONING SYSTEM (GPS) OPERATIONAL CONTROL SEGMENT (OCS) ESTIMATION AND OTHER APPLICATIONS.

Conference paper published in the Proceedings of the Institute of Navigation - 20th International Technical Meeting of the Satellite Division, ION GNSS 2007, held September 2007 in Fort Worth, TX.

PAO Case Number: SN 07-0176; Clearance date: 07 May 2007. The U.S. Government is joint author of this work and has the right to use, modify, reproduce, release, perform, display, or disclose the work. Paper contains color.

14. ABSTRACT
A new approach to weak GPS signal acquisition is presented in this paper. It belongs to the category of approaches that aim at enhancing the sensitivity of standalone GPS receivers without network assistance, which is also called unaided GPS receivers.

Acquisition and ultimate tracking of a weak GPS signal (e.g., in an in-door environment) faces several technical challenges, notably, possible data bit sign reversal every 20 ms and tolerable frequency error inversely proportional to the integration interval. Brute force search over all possible combinations of the unknown values is prohibitive computationally. Aided GPS relying on external infrastructure for timing, data bit, and frequency error information is costly. *Abstract concludes on reverse side →*

15. SUBJECT TERMS

16. SECURITY CLASSIFICATION OF:			17. LIMITATION OF ABSTRACT:	18. NUMBER OF PAGES	19a. NAME OF RESPONSIBLE PERSON (Monitor)
a. REPORT	b. ABSTRACT	c. THIS PAGE			Thao Nguyen
Unclassified	Unclassified	Unclassified	SAR	16	19b. TELEPHONE NUMBER *(Include Area Code)* N/A

14. ABSTRACT (concluded)

Coherent techniques such as the block accumulating coherent integration over extended interval (BACIX) have recently been proposed to extend coherent integration. Although efficient, such coherent methods may still be too expensive except for high-end receivers and may not maintain the SNR performance when there are large frequency changes over the intended integration interval.

In this paper, we set forth a novel method that utilizes the semi-coherent scheme for post-correlation integration, which is named as "block accumulating semi-coherent integration of correlations" or BASIC. It can be viewed as an extension of the BACIX algorithm. Although less sensitive than coherent integration, semi-coherent integration based on inter-block conjugate products is computationally more efficient. In addition, it can handle large frequency changes.

The BASIC algorithm is first formulated in the paper. Computer simulation results are then presented to illustrate operation and performance of the BASIC algorithm for joint estimation of the initial frequency, chirping rate (frequency rate), bit sync, and bit sign pattern.

Wigner-Hough/Radon Transform for GPS Post-Correlation Integration

Dr. Chun Yang	*Sigtem Technology, Inc.*
Dr. Mikel Miller	*Air Force Research Lab/MNG*
Dr. Thao Nguyen	*Air Force Research Lab/RYRN*
Dr. Erik Blasch	*Air Force Research Lab/RYAA*

BIOGRAPHIES

Dr. Chun Yang received his title of Docteur en Science from the Université de Paris (No. XI, Orsay), France, in 1989. After two years of post-doctoral research at the University of Connecticut, he moved on with his industrial R&D career. Since 1993, he has been with Sigtem Technology, Inc. and has been working on numerous GPS, integrated inertial, and adaptive array related projects. He is the co-inventor of seven issued or pending U.S. patents. He is also an Adjunct Professor of Electrical and Computer Engineering at Miami University of Ohio.

Dr. Mikel Miller is the Technical Director for Advanced Guidance Division, Munitions Directorate, Air Force Research Laboratory, Eglin AFB, FL. He received his Ph.D. in Electrical Engineering from the Air Force Institute of Technology (AFIT), WPAFB, Ohio, in 1998. Since 1986, he has focused on navigation system R&D related to GPS, GPS/INS integrations, alternative navigation techniques including bio-inspired navigation and signals of opportunity based navigation, autonomous vehicle navigation and control, and multi-sensor fusion. He is currently responsible for directing both in-house and contracted R&D projects advancing weapon system GNC technology. He is also an Adjunct Professor of EE at AFIT and Miami University of Ohio. Dr. Miller is a member of the ION, RIN, IEEE, and AIAA.

Dr. Thao Nguyen received his Ph.D. in the Electrical Engineering from the Air Force Institute of Technology (AFIT), Wright-Patterson AFB, Ohio, in 2007. He also works as an Electronics Engineer at the Reference Systems Branch, Sensors Directorate, Air Force Research Laboratory, WPAFB, OH. Dr. Nguyen has been involved in navigation-related research, development, and test since 2002 and his current areas of interest include high anti-jamming technologies for GPS receivers, GPS/INS integration, multi-sensor fusion, and personal navigation using signals of opportunity (SoOP).

Dr. Erik Blasch is a Fusion Evaluation Tech Lead for the Assessment & Integration Branch, Sensors Directorate, Air Force Research Laboratory, WPAFB, OH. He is an adjunct professor at Wright State University (WSU)/ University of Dayton (UD)/AFIT and a Reserve Major at the Air Force Office of Scientific Research (AFOSR). He received his Ph.D. in Electrical Engineering from WSU in 1999, a MSEE from WSU in 1997, a MSME from Georgia Tech in 1994, and a BSME from MIT in 1992 among other advanced degrees in engineering, health science, economics, and business administration. He is the President of the International Society of Information Fusion (ISIF) and active in IEEE, SPIE, and ION. His research interests include target tracking, sensor fusion, automatic target recognition, biologically-inspired robotics, and controls.

ABSTRACT

This paper investigates the application of the Wigner-Hough transform (WHT) or Wigner-Radon transform (WRT) and their variants to GPS post-correlation integration. For an acquisition scheme wherein frequency search step is 500 Hz and code search step is a half chip, GPS despreading correlation is typically carried out over 1 millisecond. Such integration at the rate of 1 kHz can tolerate ±250 Hz errors in frequency and ±¼ chips in code phase in the sense of 3 dB loss of correlation power. In many applications, it is desired to integrate the 1 ms correlations over a rather long period of time so as to boost the signal strength while averaging out noise and interference. When the integration interval extends to and beyond 20 ms, the signs of data bits have to be considered. For even longer intervals, changes in signal frequency due to motion-induced Doppler and/or clock drift become important and have to be taken into account.

Under a constant acceleration, the complex correlations are subject to a varying Doppler frequency, which behaves like a chirp signal (a linear frequency modulation or LFM). The Wigner-Ville distribution (WVD) is a well known method to estimate instantaneous frequency, which appears as a straight line in the time-frequency plane. The Hough transform (HT) is another well-known method to detect a line, which can be used to integrate the chirp signal power along the line. Similar to the HT, the Radon transform (RT) is another formulation that evaluates integrals along straight lines. However, the combination of the WVD and HT (called the Wigner-Hough transform) or the combination of the WVD and Radon transform (called the Wigner-Radon transform), cannot be applied directly to the despread correlations because of the presence of unknown data bits.

A block-implemented WHT/WRT using the intra-block conjugate products is set forth in this paper, which can be used to estimate the initial frequency, chirping rate (frequency rate), and bit sync. Simulation results are presented to illustrate the operation and performance of the method.

INTRODUCTION

In [Yang *et al*., 2007], six post-correlation integration schemes are comparatively studied with computer simulation. These six schemes are (1) Ideal Coherent, (2) Practical Coherent with FFT, (3) Non-Coherent, (4) Semi-Coherent for First Lag with FFT, (5) Semi-Coherent for First Lag, and (6) Semi-Coherent up to First *N*/2 Lags, which are illustrated in Figure 1.

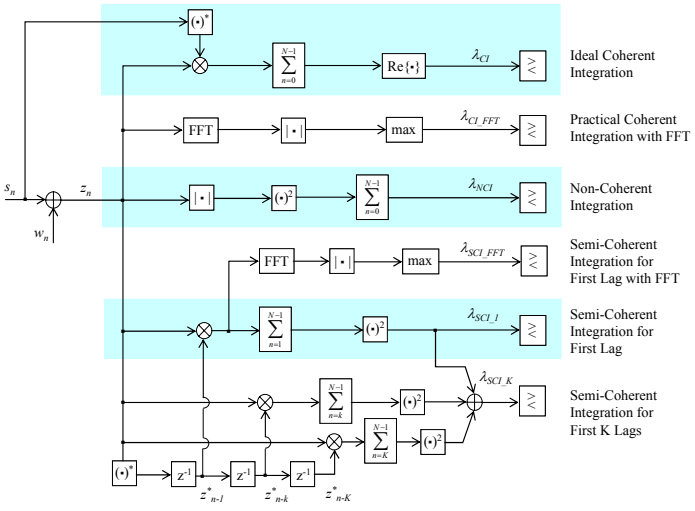

Fig. 1 – Block Diagram of Six Integration Schemes

When the change in carrier frequency is small, the six integration schemes are ranked for the SNR required to achieve the same probability of detection for a given probability of false alarm. The performance ranking has the following order:

Ideal Coherent >
Practical Coherent with FFT >
Semi-Coherent up to First N/2 Lags >
Semi-Coherent for First Lag >
Semi-Coherent for First Lag with FFT >
Non-Coherent

However, the performance of four integration schemes, except for the coherent and non-coherent schemes, starts to deteriorate when the change in carrier frequency is large, as caused by motion-induced Doppler frequency shift and clock instability and drift. The effect is especially pronounced when a long integration interval is used in order to cumulate the enough signal strength while attenuating noise.

One way to model large change in frequency is to use a quadratic phase function or a linear frequency modulation (LFM) where the frequency change rate is constant. LFM is widely used in radar signal design, which produces the so-called chirp signal with wide instantaneous bandwidth to improve range resolution [Wirth, 2001; Yang and Blasch, 2007]. It can also be used to model a variety of phenomena encountered in radar signal processing. One example is the phase variation in the cross range of a synthetic aperture radar (SAR). It is fairly accurate to model short-term phase change with a chirp signal.

Since the chirping rate is unknown but within a certain range, one technique would call for a bank of processors, each tuned to a discretized chirping rate in the range (thus dechirping) [Li, 1987]. Each of the parallel processors can implement one of the six integration schemes above mentioned. This is tantamount to a two-dimensional (2D) search, one in the chirping rate and the other in the initial frequency with FFT used for integration. The use of an adaptive filter to implement 2D search is reported in [Wang, Xia, and Chen, 1993].

There are many methods available in the digital signal processing literature for estimating a chirp signal's parameters (*i.e.*, the initial phase, initial frequency, and chirping rate) and one method of particular interest is the Wigner-Hough transform (WHT) [Barbarossa, 1996]. In this method, the Wigner-Ville distribution (WVD) is used to represent the signal energy in the time-frequency plane while the Hough transform (HT) integrates the energy belonging to a chirp signal, which is distributed along a line in the time-frequency plane. Similarly, the Radon transform can be used in place of the Hough transform to integrate the chirp energy along a line in the time-frequency plane [Wood and Barry, 1994].

In this paper, we investigate the application of the WHT or WRT and their variants to GPS post-correlation integration. For an acquisition scheme wherein frequency search step is 500 Hz and code search step is a half chip, GPS despreading correlation is typically carried out over 1 millisecond (ms) [Parkinson and Spilker Jr., 1996; Tsui,

2000; Misra and Enge, 2001; Kaplan and Hegarty, 2006]. Such integration at the rate of 1 kHz can tolerate ±250 Hz errors in frequency and ±¼ chips in code phase in the sense of 3 dB loss in correlation power. In many applications, it is desired to further integrate the 1 ms correlations over a rather long period of time. When the integration interval extends to and beyond 20 ms, the signs of data bits have to be considered in addition to changes in signal frequency [Yang and Han, 2006].

However, the combination of the WVD and HT, called the Wigner-Hough transform (WHT), or the combination of the WVD and RT, called the Wigner-Radon transform (WHT), cannot be applied directly to the despread correlations because of the presence of unknown data bits. We set forth a block-implemented WHT/WRT using the intra-block conjugate products in this paper. They can be used to jointly estimate the initial frequency, chirping rate (frequency rate), and bit sync. After introducing a complex model for post-correlation GPS signals, we present the Wigner-Hough transform and Wigner-Radon transform. We then describe a variant of the WHT or WRT based on intra-block conjugate products together with simulation results to illustrate the operation and performance. Finally, a summary is provided with concluding remarks and future work.

COMPLEX MODEL FOR POST-CORRELATION GPS SIGNALS

Consider a scheme for acquiring GPS signals via search in time and frequency. Assume that the frequency search step is 500 Hz, the code search step is half a chip, and the integration interval of the despreading correlation is 1 ms. Such integration can tolerate ±250 Hz errors in frequency and ±¼ chips. The resulting complex correlation is unique for each GPS satellite and can be written as:

$$x_n = b_n A_n \exp\{j[2\pi(f_0 n T_s + \alpha n^2 T_s^2) + \phi_0]\} + w_n \qquad (1)$$

where x_n is the complex post-correlation signal with the sample index n, A_n is the amplitude, ϕ_0 is the initial phase, T_s = 1 ms is the despreading integration interval with the sampling rate of 1 kHz, $b_n = \pm 1$ is the unknown data bit, f_0 is the initial frequency, α is the chirping rate (sometimes $\alpha/2$), and w_n is an uncorrelated noise with zero mean and unity variance.

For GPS C/A-codes, the baud rate is 50 Hz and the data bit thus has a periodicity of 20 ms. There will be 20 samples per data bit of the same sign, but it may change sign from one data bit to the next. Knowing which sample is the start of a data bit is the bit synchronization or bit sync process. Without knowing the bit sync, a perfect correction may be destroyed if there is a data bit sign reversal in the middle of integration. It is equally important to determine the sign of data bits, from which the navigation messages can be demodulated.

The instantaneous frequency in Eq. (1) represents the frequency error between the incoming signal and the local carrier replica, which can be written as:

$$\Delta f_n = f_0 n T_s + \alpha n^2 T_s^2 \qquad (2)$$

For the local carrier replica fixed at a search frequency, the complex model in Eq. (1) is useful as long as the frequency error, albeit being time-varying, remains within ±250 Hz. Otherwise, the search switches to another search frequency. Over a time interval of T_i, the maximum chirp rate for a fixed carrier replica is:

$$\alpha = -sign(f_0)\frac{500 - |f_0|}{T_i} \qquad (3)$$

where $sign(\blacksquare)$ is a sign function, so that the change in frequency is less than 500 Hz in one second. The maximum chirp rate is therefore α = 500 Hz/s. At L1 = 1575.42 MHz, the frequency change over one second is related to the underlying acceleration (in g = 9.8 m/s^2) by the factor of 51.49 Hz/g/s.

The signal amplitude A_n includes a factor $R(\Delta\tau)$ related to timing error $\Delta\tau$, where $R(\blacksquare)$ is the correlation function for the GPS spreading code, and a factor $\sin(\pi T_s \Delta f)/\pi T_s \Delta f$ related to frequency error Δf [Parkinson and Spilker, 1996; Tsui, 2000; Misra and Enge, 2001; Kaplan and Hegarty, 2006]. As a result, the signal amplitude A_n is also subject to variations due to changes in Δf. Since the change is rather small, the amplitude is assumed to be constant for simplicity in this paper.

In many applications, it is desired to further integrate the 1 ms correlations, x_n, over a rather long period of time, T_i. Because of the unknown data bits b_n and varying frequency errors Δf, it is counter-productive to sum complex correlations x_n directly. Squaring can move both the data bit and the unknown frequency error and allows for direct summation. However, this non-coherent integration also squares noise [Yang *et al.*, 2007] and further strips off all valuable information about the signal that is needed for subsequent processing in a GPS receiver.

WIGNER-HOUGH AND WIGNER-RADON TRANSFORMS

The post-correlation GPS signal as modeled in Eq. (1) is a chirp signal with a linear frequency modulation. The instantaneous frequency is characterized by two parameters, namely, the initial frequency f_0 and the chirping rate α. The Wigner-Ville distribution is a popular method to represent the signal energy in the time-frequency plane [Flandrin, 1999]. It obtains the signal energy distribution by applying the Fourier transform to the centered autocorrelation function (CAF) of a time-varying signal.

For a continuous-time signal $x(t)$, its Wigner-Ville

distribution or WVD is computed as:

$$W(t,f)=\int_{-\infty}^{+\infty}x(t+\frac{\tau}{2})x^*(t-\frac{\tau}{2})e^{-j2\pi f\tau}d\tau \quad (4)$$

where * stands for complex conjugate. A window function is typically applied so as to restrict the integral limits to a finite length. With $t = nT_s$, $\tau = mT_s$, and $f = k/(N+1)T_s$, the discrete version of the Wigner-Ville distribution (DWVD) can be written as:

$$W(n,k)=2\sum_{m=-N/2}^{N/2}x(n+m)x^*(n-m)\exp(-j4\pi mk/(N+1)) \quad (5)$$

where the total number of samples analyzed is $N+1$.

In addition to discrete time steps, the discrete distribution also has discrete frequency steps. This may be perceived as a limitation when there are closely spaced signals to resolve. For a fixed sampling rate, one way to reduce the frequency step is to zero-pad the data samples beyond N. Interpolation can also be used to obtain an "increased" sampling rate. This is a tradeoff between computation and resolution. The selection of a window function is another important design issue that can be used to suppress cross terms when multiple chirp components are present in the signal.

The Hough transform (HT) is a popular digital image processing technique widely used to find a straight line from an image [Duda and Hart, 1972]. For a polar coordinate system with its origin at the center of the image, a line can be represented by two parameters, $r \geq 0$ and $\theta \in [0, 2\pi)$, where θ is the angle between the x-axis and the origin-passing perpendicular to the line and r is the length from the origin to the intercept of the perpendicular to the line (the closest point). The line can be written as:

$$L_{\theta r}:\ (\theta,\quad r)=(\theta,\quad r=x\cos\theta+y\sin\theta) \quad (6)$$

For a single point (x, y) in the image plane, there are an infinite number of lines go through this point, each corresponding to a sinusoidal curve given by Eq. (6) in the (θ, r) plane. For a set of points that form a straight line, their sinusoidal curves cross at the parameters for that line in the (θ, r) plane. The number of curves that cross at the same point in the (θ, r) plane is the number of the image points that lie along the same line. Therefore, the HT thus converts a line in the original image plane into a point in the parameter plane, while integrating the image values along the line.

This description makes the Hough transform to be conceptually very close to the Radon transform (RT) [Deans, 1983]. In general, the RT calculates the integral of a function $f(x, y)$ over the set of all lines, each characterized by two parameters in the polar coordinates (θ, r). In the x-y plane, a line is represented by the set of all points along the line:

$$L_{xy}:\ (x,\quad y)=(-\infty<x<\infty,\quad y=\sin^{-1}\theta(r-x\cos\theta)) \quad (7)$$

Although the integration can be carried in the x-y plane directly using Eq. (6), it is not convenient particularly with possible singularities (θ = 90 or 270 degrees). An easy implementation consists of rotate the x-y plane by θ into the ξ-η plane and then integrates along the line, which is now parallel to the η-axis defined as ($\xi = r$, $-\infty < \eta < \infty$), as illustrated in Figure 2. The Radon transform can now be written as:

$$Rf(\theta,r)=\int_{l\in L_{xy}}f(x,y)dl$$

$$=\int_{-\infty}^{\infty}f(\xi\cos\theta-\eta\sin\theta,\xi\sin\theta+\eta\cos\theta)d\eta,\ \xi=r \quad (8)$$

It has been shown that the Radon transform performs better than the Hough transform to detect lines when an image is corrupted by speckle because noise can be effectively attenuated in the Radon transform with explicit summation along lines.

Clearly, both the HT and RT also involve selection of discrete steps for r and θ. There will be quantization errors, which again is a tradeoff between computation and resolution.

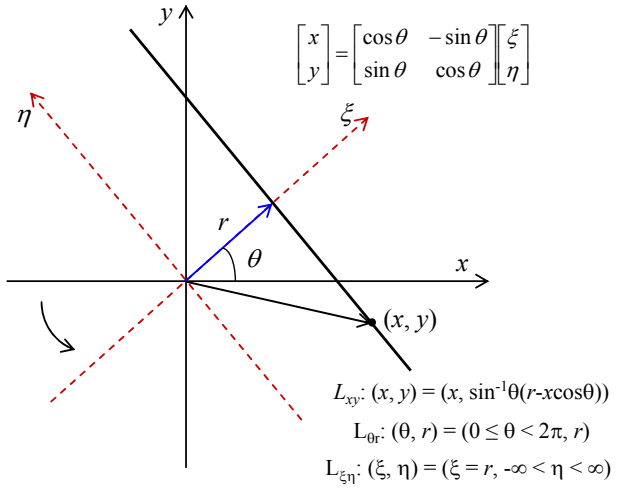

Fig. 2 – Integration Path for Hough and Radon Transforms

When the Hough transform/the Radon transform is applied to the Wigner-Ville distribution, the Wigner-Hough transform/the Wigner-Radon transform results, which can integrate the energy belonging to a chirp signal along a line in the time-frequency plane. The chirp parameters are therefore obtained as:

$$(\hat{f}_0,\hat{\alpha})=\arg\max_{f_0,\alpha}\int W(t,f_0+\alpha t)dt \quad (9a)$$

$$=\iint x(t+\frac{\tau}{2})x^*(t-\frac{\tau}{2})e^{-j2\pi(f_0+\alpha t)}dtd\tau \quad (9b)$$

where both integrals are limited to some observation interval.

Since the WVD is a density function of signal energy over the time-frequency plane, when integrating along all lines in the WD, Eq. (9) provides the maximum likelihood (ML) estimates of the linear FM signal parameters in white Gaussian noise.

The basic ideas of the Wigner-Ville transform and the Hough transform or the Radon transform described in this section are applied in the following sections for integrating the post-correlation GPS signal subject to unknown Doppler changes and data bits.

WHT/WRT WITH INTRA-BLOCK CONJUGATE PRODUCTS

As modeled in Eq. (1), the post-correlation signal is available at a rate of 1 kHz. Our goal is to integrate a large number of post-correlation signals x_n, for n = 1, …, N, in the presence of the unknown frequency f_0, chirping rate α, and data bits b_n. Consider an integration interval of 1 s when N = 1000 for T_s = 1 ms. To deal with unknown data bits, the N consecutive signal samples are grouped into K blocks; each block will contain M complex correlations such that $N = KM$. A block of data is denoted by a vector $\underline{y}_k = [x_{20(k-1)+i}, \quad i = 1,...,M] = [x_{ki}, \quad i = 1,...,M]$. When M = 20, a block will last 20 ms, which is the duration of a data bit for GPS C/A-codes.

To facilitate presentation, we omit the terms related to noise in the derivation. Referring to Fig. 3, we re-label the time index of each sample in a block relative to the block center by $t \pm \tau/2$ where t is the time of the block center in units of MT_s and $\tau/2$ = 0.5, 1.5, …, 9.5 in units of T_s. The centered autocorrelation between two samples with delay τ is given by:

$$z(t,\tau) = x(t+\frac{\tau}{2})x^*(t-\frac{\tau}{2}) \tag{10a}$$

$$= A^2 e^{j2\pi(f_0+2\alpha t)\tau},$$

$$\tau = \pm 1, \quad \pm 3, \quad \cdots, \quad \pm M-1, \; t = 1, \quad 2, \quad \cdots, \quad K \tag{10b}$$

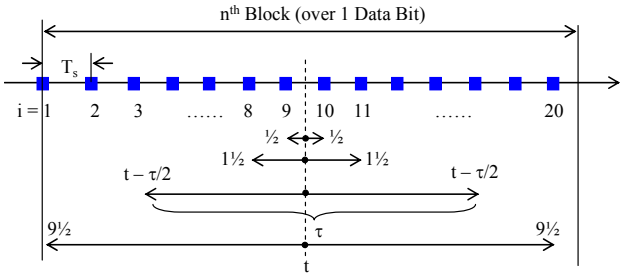

Fig. 3 – Time Diagram for Intra-Block Conjugate Products

To arrive at Eq. (10b), it is assumed that the two samples share the same data bit, that is, $b(t+\tau/2)b(t-\tau/2) = (\pm 1)^2 = 1$. The aspect of bit sync will be addressed later in this section.

If the signal is strong enough, the fast Fourier transform (FFT) can be applied to $z(t, \tau)$ over τ for each block t and the results are denoted by:

$$Z(t,f) = \mathcal{F}_\tau\{[(z(t,\tau), \quad \tau = -M+1,...,-3,-1,1,3,...,M-1), \quad \underline{0}_{\mu M}]\} \tag{11}$$

where $\mathcal{F}_\tau\{\bullet\}$ stands for the FFT applied along the dimension τ, $\underline{0}_n$ is a vector of n zeros, and μ is the factor of M zeros padded to $z(t, \tau)$ prior to the FFT.

The peak location of $Z(t, f)$ will provide an estimate of the quantity $f_0 + 2\alpha t$. Repeating this operation for all blocks yields the time-frequency distribution of the signal energy, which forms a straight line starting at f_0 and moving at the slope of 2α as shown in Fig. 4. This is in fact the basic idea behind the Wigner-Ville transform given in Eq. (4), which then requires search in two unknowns, f_0 and α, while integrating the signal energy using either the Hough transform or Radon transform as discussed in the previous section. As shown in Fig. 4, the estimates of the unknowns are taken as those that maximize the resulting sum $S(f_0, \alpha)$:

$$(\hat{f}_0, \hat{\alpha}) = \arg\max_{f_0,\alpha} S(f_0,\alpha) \tag{12a}$$

$$S(f_0,\alpha) = \sum_{\substack{f=f_0+2\alpha t \\ t\in[1,...,K]}} Z(t,f) \tag{12b}$$

where the arguments are converted from r and θ to f_0 and α.

Alternatively, the FFT can be taken on $z(t, \tau)$ over t for each τ, denoted by:

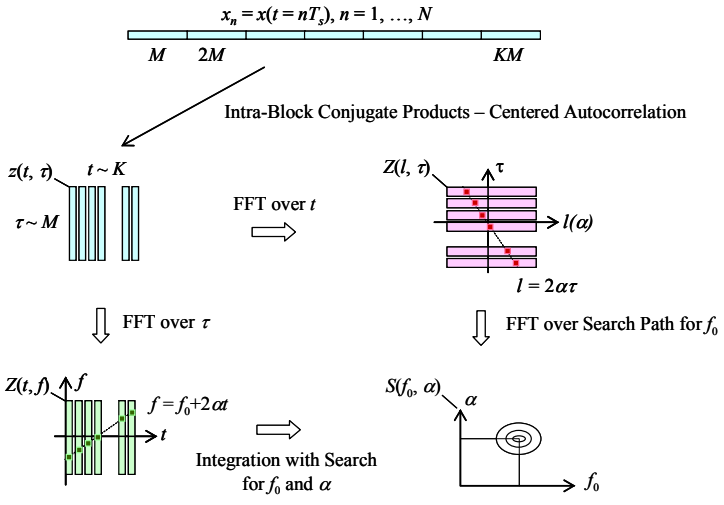

Fig. 4 – Relationship between Various Transforms

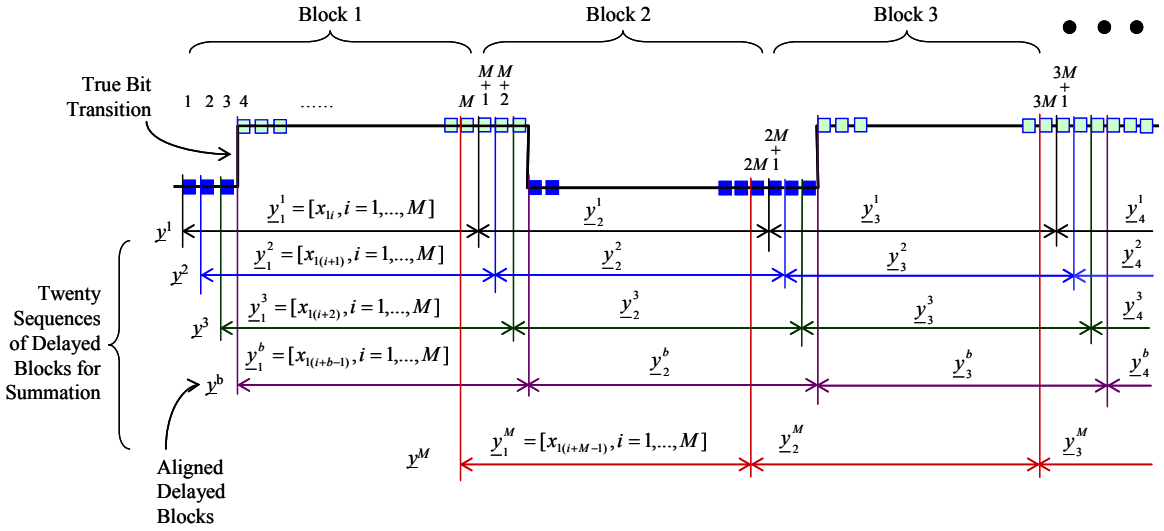

Fig. 5 – Twenty Delayed Sums for Bit Sync

$$Z(l,\tau) = \mathcal{F}_t\{[(z(t,\tau), \quad t = 1,2,...,K), \quad \underline{0}_{\kappa K}]\} \tag{13}$$

Alternatively, the FFT can be taken on $z(t, \tau)$ over t for each τ, denoted by:

$$Z(l,\tau) = \mathcal{F}_t\{[(z(t,\tau), \quad t = 1,2,...,K), \quad \underline{0}_{\kappa K}]\} \tag{13}$$

As shown in Fig. 4, the peak location of $Z(l, \tau)$ within $\pm(\kappa+1)K/2$ is obtained as:

$$\hat{l}(\tau) = \arg\max_{l} |Z(l,\tau)| \tag{14}$$

$\hat{l}(\tau)$ provides an estimate of the quantity $2\alpha\tau$. With τ known, the chirping rate α can be estimated directly as:

$$\hat{\alpha}(\tau) = \frac{1}{2}\frac{\hat{l}(\tau)}{\tau T_s^2 N(\kappa+1)} \tag{15}$$

Another advantage of this approach is that the number of blocks K can be increased as more data become available (and for possible recursive implementation) whereas the number of delays M is limited per data bit duration. When the signal is strong enough, the peak values $Z(\hat{l}(\tau), \tau) = KA^2 e^{j2\pi f_0\tau}$ can be further FFT-analyzed over τ and the location of the peak of this second FFT provides an estimate of the initial frequency f_0.

When the signal is not strong enough to ensure reliable detection of peaks of in $Z(l, \tau)$, search for the signal path (l, τ) is required. Again, there are quantization errors in defining the search path, which may be reduced to some extent by zero-padding. For each α, the peak location l is a well-defined linear function of τ. As a result, the search is one dimensional. The FFT is used to integrate along the selected path, leading to $S(f_0, \alpha)$ given by:

$$S(f_0,\alpha) = \mathcal{F}_\tau\{[Z(l,\tau), \quad l = 2\alpha\tau, \quad \tau = 1,...,\mu M]\} \tag{16}$$

where the arguments are converted to f_0 and α as shown in Fig. 4. The signal parameters are estimated using Eq. (12a) as those that maximize $S(f_0, \alpha)$ defined in Eq. (16)

In the above derivations, it is assumed that the two samples of a block involved in the conjugate product share the same data bit sign such that $b(t+\tau/2)b(t-\tau/2) = (\pm1)^2 = 1$. This implies that this block is perfectly aligned (or bit synchronized – bit sync) with data bits. For practical implementation, however, the parameter estimation has to be performed at the same time as the bit sync. One simple approach to bit sync is to maintain twenty sums of blocks. The start of blocks of a sum corresponds to a possible bit transition location within 20 ms and the block in one sum is delayed by one sample (1 ms) relative to the preceding sum, as illustrated in Fig. 5.

The k^{th} block in the b^{th} sum is therefore constructed as:

$$\underline{y}_k^b = [x_{20(k-1)+i+b-1}, \quad i = 1,...,20],$$
$$b = 1, \ldots, 20, \; k = 1, \ldots, K \tag{17}$$

The method of Eq. (16) can be applied to each of the twenty sums over K blocks, denoted by $S^b(\underline{y}_n^b, n = 1, \ldots, K)$. The sum that produces the maximum value provides an estimate of the data bit transition (*i.e.*, the tentative bit sync) as:

$$\hat{b} = \arg\max_b S^b(\underline{y}_1^b,...,\underline{y}_n^b,...,\underline{y}_K^b) \tag{18}$$

SIMULATION RESULTS AND ANALYSIS

Simulation examples are presented below to illustrate the operation and performance of the method using intra-block conjugate products for joint signal parameter estimation and bit sync. In the first simulation example, we consider an ideal case where there is no noise and no data modulation. The integration interval is 1 s with $N =$

1000 for T_s = 1 ms. The data are divided into K = 50 blocks, each with M = 20 samples. The initial phase is θ = 32°, the initial frequency is f_0 = -250 Hz, and the chirping rate is $\alpha/2$ = 250 Hz/s.

Fig. 6 shows the amplitude spectrum of the FFT applied to the intra-block conjugate products, $Z(l, \tau)$, as given in Eq. (13) where κ = 3. The length of the FFT is $(\kappa+1)K$ = 4×50 = 200 but the peak value is 50, equal to the length of non-zero data points K = 50. There are two groups of curves and the locations of these curve's peak correspond to $2\alpha\tau$ for $\tau = \pm 0.5, \pm 1.5, \ldots, \pm 9.5$. Because of the sign of τ, the two groups appear symmetrically in positive frequency bins (left) and negative frequency bins (right). For this ideal case, the estimated chirping rate using Eq. (15) is $\frac{1}{2}\hat{\alpha}(\tau) = 250$, correct for all τ, as shown in Fig. 7. To save computation, however, only one group of curves is in fact needed, either with positive or negative τ.

The FFT-analysis of the peaks selected from $Z(l, \tau)$ for τ = 1, …, μM is equivalent to integrating along the signal path. As shown in Fig. 8, the peak location corresponds to the initial frequency f_0. For this case with μ = 3 and M = 20, the FFT length is $(\mu+1)M$ = 80. The frequency estimate corresponding to the peak at 41 is (41-80)*6.25 = -243.75 Hz, which is quite close to the true value of f_0 = -250 Hz without interpolation.

The FFT integration in Fig. 8 is done along a special path, which is determined by picking the peaks at $(l(\tau), \tau)$, τ = 1, …, μM. Without peak detection, the signal path can be searched using Eq. (16). The results are shown in Fig. 9. For this ideal case, the estimated chirp rate is 250.00 Hz/s (vs. $\alpha/2$ = 250 Hz/s), the initial frequency at the peak value is -237.50 (vs. f_0 = -250 Hz), and the peak value is 947.92 (vs. the full value of 1000) without interpolation.

In the second simulation example, all the conditions are kept same as in the first simulation example except complex noise is added such that the resulting signal to noise ratio is SNR = -3 dB. Under the Nyquist rate, the signal passes through a low pass filter with an equivalent bandwidth of $\pm f_s/2$. For T_s = 0.001 s, SNR = -3 dB results from A = 0.7, which also corresponds to C/N_0 = 27 dB-Hz.

Fig. 10 shows the amplitude spectrum of the FFT applied to the intra-block conjugate products along k. Compared to the ideal case in Fig. 6, there are only few peaks that can be reliably detected for this low SNR case. But the spectrum is still symmetric, indicating that only half of delays (either positive or negative τ) would be needed. The use of more delays did not necessarily reduce noise.

It is then not a surprise to see from Fig. 11 that the chirping rate estimates per τ are quite noisy except for those strong peaks in Fig. 10. In particular, those estimates for small τ's are erroneous. Nevertheless, Fig. 12 shows the FFT integration along the path determined by the peaks of Fig. 10, which produces the initial frequency estimate rather correctly. As compared to Fig. 8, the noise floor is however raised and the peak is lowered in Fig. 12.

Instead of picking peaks from Fig. 10, which is not reliable for low SNR, search is done over possible chirping rates, each specifying a particular path to integrate using Eq. (16). The results are shown in Fig. 13. Compared to Fig. 9, the noise floor is raised and the peak is lowered. Without interpolation, the estimated chirp rate is 237.00 Hz/s (vs. $\alpha/2$ = 250 Hz/s), the initial frequency at the peak value is -237.50 (vs. f_0 = -250 Hz), and the peak value is 394.41 (vs. the value of 947.92 in the noise-free case).

In the third simulation example, data bits are modulated onto the signal samples. In the example, the first bit transition occurs between the 16th and 17th samples. In other words, the 16th sample is the end of the first incomplete data bit and the 17th sample is the start of a second data bit. Fig. 14 shows the twenty delayed sums at K-1 for the ideal case, from which Eq. (18) can be applied to determine the bit sync at 17th. Fig. 15 shows the twenty delayed sums for SNR = -3 dB. The presence of noise has not lowered much the peaks for those sums that hypothesized bit transitions near b = 7. For this example, sums starting at those samples placed the bit transitions in the middle of integration, thus rending it noise like. This explains why adding another noise term did not change much. However, the peaks for those sums that are near b = 17 have been reduced in magnitude nearly by half for SNR = -3 dB. Nevertheless, it is clearly possible and reliable to detect the cumulated peak corresponding to the true bit transition, thus achieving bit sync.

The product of two samples within a block effectively eliminates the sign of data bits, thus making integration across blocks possible. However, other means have to be used to determine the data bit signs from which to demodulate any message that may be embedded. One method using inter-block conjugate products that allows for joint signal parameter estimation and bit sync as well as bit sign determination will be presented in [Yang et al., 2008].

CONCLUSIONS

In this paper, the GPS signal after the 1 ms despreading integration was modeled as a modulated chirp signal. This model is useful even in the acquisition mode where search is conducted at a frequency step of 500 Hz and a code lag of ½ chips. In this model, the binary modulation represents the data bits of navigation message while the chirp accounts for changes in residual Doppler frequency.

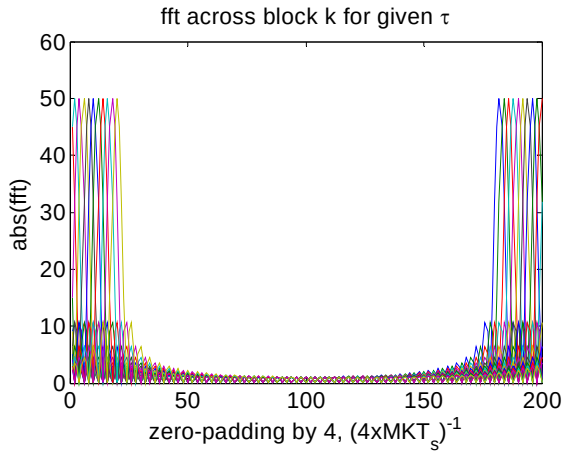

Fig. 6 – FFT over k for Given τ

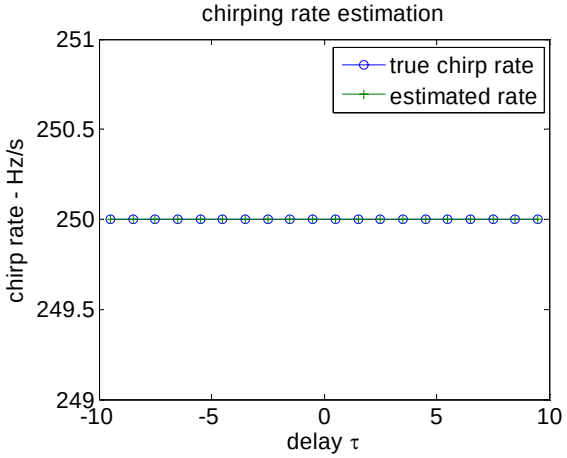

Fig. 7 – Chirping Rate Estimation per τ

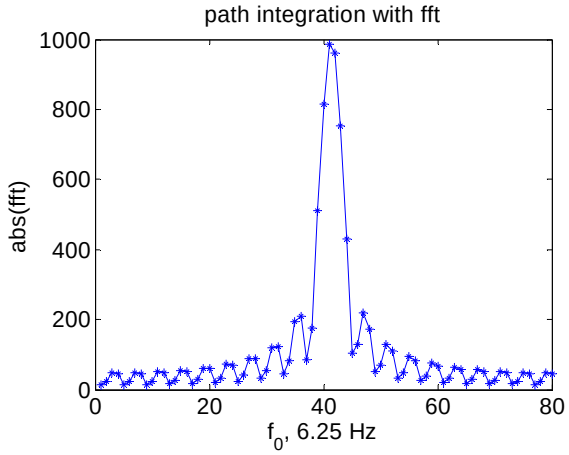

Fig. 8 – Initial Frequency Estimation

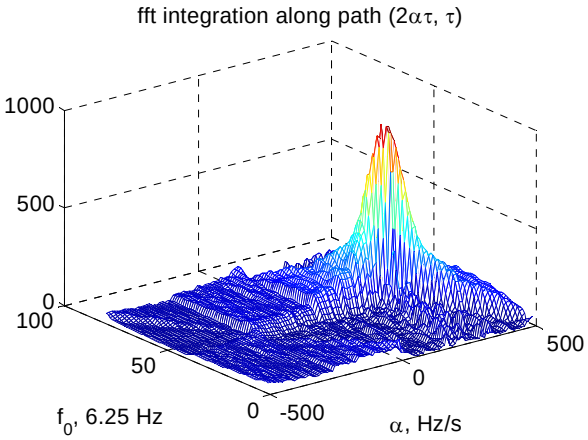

Fig. 9 – FFT Integration along Search Path

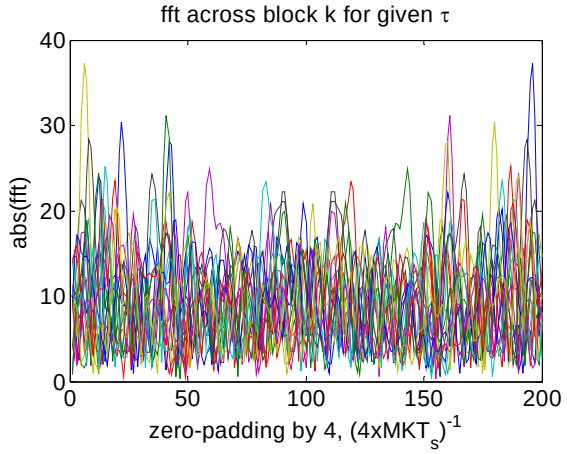

Fig. 10 – FFT over k for Given τ for SNR = -3 dB

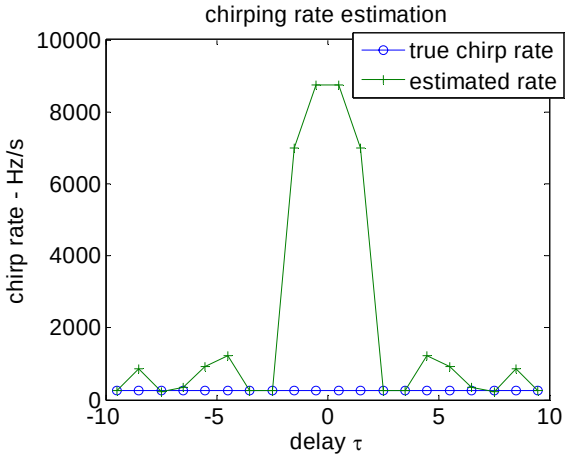

Fig. 11 – Chirping Rate Estimation per τ for SNR = -3 dB

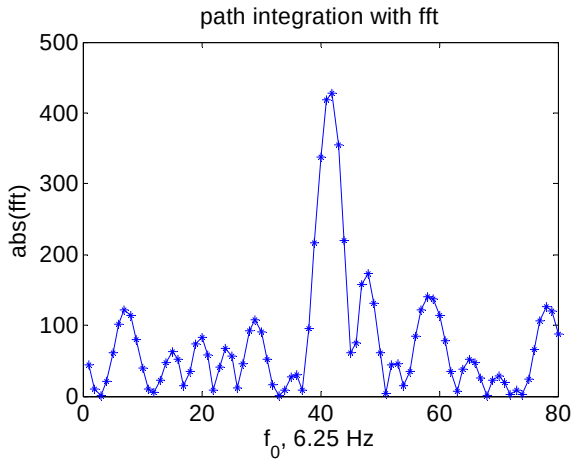

Fig. 12 – Initial Frequency Estimation for SNR = -3 dB

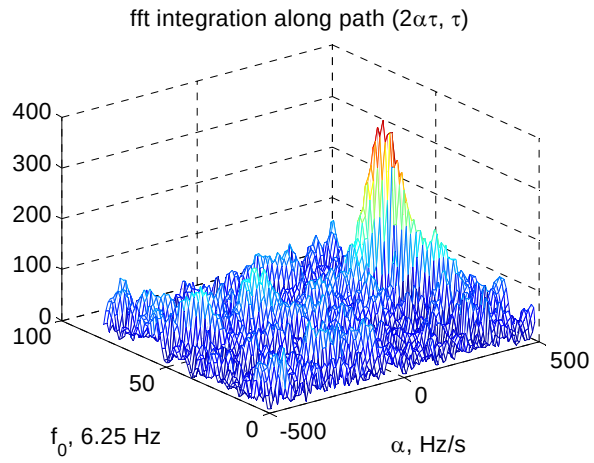

Fig. 13 – FFT Integration along Search Path for SNR = -3 dB

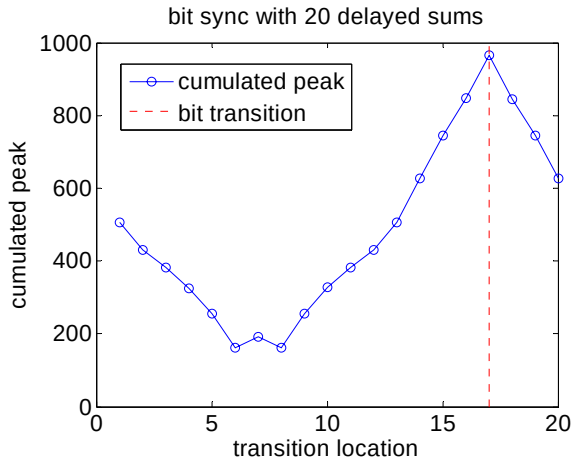

Fig. 14 – Cumulative Peaks for Bit Sync

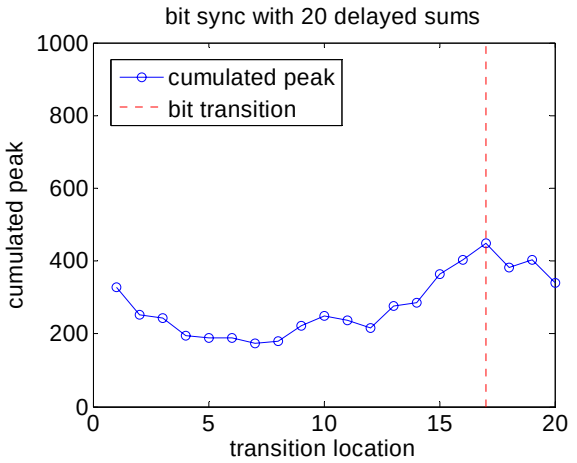

Fig. 15 – Cumulative Peaks for Bit Sync for SNR = -3 dB

To further integrate the signal, a new method was presented based on the basic ideas of the Wigner-Ville transform (delayed conjugate products) and the Hough or Radon transform (integration along a linear path). The method was based on the intra-block conjugate products and so designed for jointly estimating the signal parameters (i.e., the initial frequency and chirping rate) and data bits (bit sync). Simulation results were presented and illustrated the operation and performance of the method.

The block-integrating methods presented in this paper can handle large frequency changes as caused by relative motion and clock drift. It can also remove data bits in an open-ended manner, allowing for new samples to be added on in the integration process as they become available. These and other features make it suitable for such applications as in high dynamics and/or weak signal environments. Beyond naturally occurring changes in Doppler frequency, modulated chirping signal may be used for signaling in special CDMA applications and MIMO radar for detection of stealthy targets among others.

ACKNOWLEDGMENTS

Research supported partially under Contracts No. FA8650-05-C-1808 and FA8650-05-C-1828, which are gratefully acknowledged.

REFERENCES

S. Barbarossa, "Analysis of Multicomponent LFM Signals by a Combined Wigner-Hough Transform," *IEEE Trans. on Signal Processing*, 43(6), June 1995.

S.R. Deans, *The Radon Transform and Some of Its Applications*, John Wiley & Sons, New York, 1983.

R.O. Duda and P.E. Hart, "Use of the Hough Transformation to Detect Lines and Curves in Pictures," *Comm. ACM, Vol. 15*, January, 1972.

P. Flandrin, *Time-Frequency/Time-Scale Analysis*, Academic Press, 1999.

E.D. Kaplan and C.J. Hegarty (eds.), *Understanding GPS: Principles and Applications* (2nd Ed.) Artech House Publishers, Norwood, MA, 2006.

W. Li, "Wigner Distribution Method Equivalent to Dechirp Method for Detecting a Chirp Signal," *IEEE Trans. Acoust. Speech, Signal Process.*, 35, 1987.

P. Misra and P. Enge, *Global Positioning System, Signals, Measurements, and Performance*, Ganga-Jamuna Press, 2001.

B.W. Parkinson and J.J. Spilker Jr. (eds.), *Global Positioning System: Theory and Applications*, AIAA, 1996.

J.B.Y. Tsui, *Fundamentals of Global Positioning System Receivers - A Software Approach*, John Wiley & Sons, Inc., 2000.

G.Y. Wang, X.G. Xia, and V.C. Chen, "Adaptive Filtering Approach to Chirp Estimation and Inverse Synthetic Aperture Radar Imaging of Maneuvering Targets," *Opt. Eng.*, 42(1), January 1993.

W.D. Wirth, *Radar Techniques Using Array Antennas*, IEE, London, UK, 2001.

J.C. Wood and D.T. Barry, "Linear Signal Synthesis Using the Radon-Wigner Transform," *IEEE Trans. on Signal Processing*, 42, 1994.

C. Yang and E. Blasch, "A New Method for Extended Radar Pulse Integration Subject to Large Doppler Change," *Workshop on "Radar Resolution, Nonlinear Estimation, and Other Gratuitous Remarks on the Back of Envelope: A Tribute to Fred Daum*," Monterey, May 2007.

C. Yang and S.W. Han, "Block Accumulating Coherent Integration Over Extended Interval (BACIX) for Weak GPS Signal Acquisition," *Proc. of ION-GNSS'06*, Ft. Worth, TX, September 2006.

C. Yang, M. Miller, T. Nguyen, and E. Blasch, "Comparative Study of Coherent, Non-Coherent, and Semi-Coherent Integration Schemes for GNSS Receivers," *Proc. of ION-AM'07*, Boston, MA, April 2007.

C. Yang, M. Miller, T. Nguyen, and E. Blasch, "Post-Correlation Semi-Coherent Integration for High Dynamic Weak GPS Signal Acquisition," To Be Submitted to *IEEE/ION PLANS 2008*, Monterey, CA, May 2008.